Environmental Science & Technology

Article

pubs.acs.org/est

High Quantities of Microplastic in Arctic Deep-Sea Sediments from the HAUSGARTEN Observatory

Melanie Bergmann,*[,†,∥] Vanessa Wirzberger,[‡,§,∥] Thomas Krumpen,[⊥] Claudia Lorenz,[‡] Sebastian Primpke,[‡] Mine B. Tekman,[†] and Gunnar Gerdts[‡]

[†]HGF-MPG Group for Deep-Sea Ecology and Technology, Alfred-Wegener-Institut Helmholtz-Zentrum für Polar- und Meeresforschung, Am Handelshafen 12, 27570 Bremerhaven, Germany

[‡]Department of Microbial Ecology, Biologische Anstalt Helgoland, Alfred-Wegener-Institut Helmholtz-Zentrum für Polar- und Meeresforschung, Kurpromenade, 27498 Helgoland, Germany

[§]Department of Instrumental Analytical Chemistry, University Duisburg-Essen, Faculty of Chemistry, Universitätsstrasse 5, 45141 Essen, Germany

[⊥]Climate Sciences, Sea Ice Physics, Alfred-Wegener-Institut Helmholtz-Zentrum für Polar- und Meeresforschung, Bussestraße 24, 27570 Bremerhaven, Germany

Supporting Information

ABSTRACT: Although mounting evidence suggests the ubiquity of microplastic in aquatic ecosystems worldwide, our knowledge of its distribution in remote environments such as Polar Regions and the deep sea is scarce. Here, we analyzed nine sediment samples taken at the HAUSGARTEN observatory in the Arctic at 2340−5570 m depth. Density separation by MicroPlastic Sediment Separator and treatment with Fenton's reagent enabled analysis via Attenuated Total Reflection FTIR and μFTIR spectroscopy. Our analyses indicate the wide spread of high numbers of microplastics (42−6595 microplastics kg^{-1}). The northernmost stations harbored the highest quantities, indicating sea ice as a possible transport vehicle. A positive correlation between microplastic abundance and chlorophyll *a* content suggests vertical export via incorporation in sinking (ice-) algal aggregates. Overall, 18 different polymers were detected. Chlorinated polyethylene accounted for the largest proportion (38%), followed by polyamide (22%) and polypropylene (16%). Almost 80% of the microplastics were ≤25 μm. The microplastic quantities are among the highest recorded from benthic sediments. This corroborates the deep sea as a major sink for microplastics and the presence of accumulation areas in this remote part of the world, fed by plastics transported to the North via the Thermohaline Circulation.

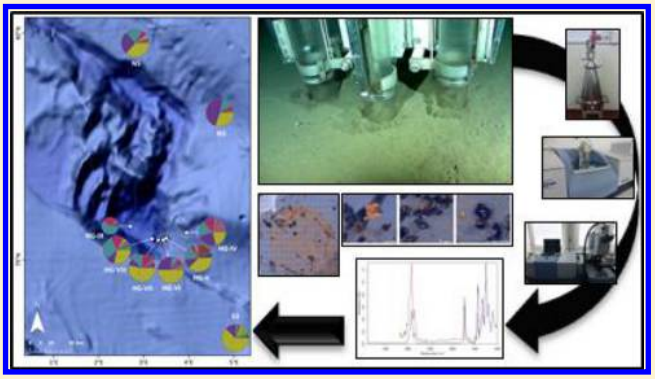

INTRODUCTION

The contamination of our oceans with plastic debris is a problem of growing environmental concern. Recently, it was estimated that 8300 million metric tons (MT) of plastics have been produced to date, 6300 MT of which have become waste as of 2015.[1] Between 4.8 and 12.7 million MT of plastic debris entered the ocean from land in 2010.[2] However, 99% of this debris have not been captured by global litter estimates.[3] It has been speculated that a large fraction of plastic debris may escape our sampling gears because of uptake and transport by biota, accumulation on the largely inaccessible deep seafloor and in other remote environments or by fragmentation into smaller particle sizes. In the marine realm, the integrity of plastics is compromised through mechanic abrasion, interaction with biota, UV radiation and temperature fluctuations such that it brittles and fragments.[4] Particles smaller than 5 mm are considered microplastics (MPs).[5] Sources for plastic in the oceans can be anthropogenic waste, which is dumped directly into the sea by fishers and other ships, aquaculture, shipyards, beach visitors, daily care products and washed-out fibers from synthetic textiles. Municipal drainage systems, road runoff and rivers represent additional entry points.[6]

Although MPs were discovered as early as in the 1970s[7] scientific research intensified only after time-series data highlighted increasing MP contamination of Atlantic waters and MP ingestion by marine biota.[8] Since then, MP has been identified in all marine realms from beaches to the deep seafloor and in all oceans and seas worldwide.[9,10] Plastic in this size range is of particular concern because it can be taken up by a wider range of biota (>172 species) and be propagated in food webs.[9] While some organisms excrete MP without any

Received: July 5, 2017
Revised: August 16, 2017
Accepted: August 17, 2017
Published: August 17, 2017

DOI: 10.1021/acs.est.7b03331
Environ. Sci. Technol. 2017, 51, 11000−11010

apparent effect,[11] in others ingested MP may interfere with food uptake and transfer adsorbed and added toxins.[9] In addition, MP between 0.5 and 438 μm may translocate to organs or blood[12−14] among other effects. Despite increased research efforts, however, the overall ecological consequences of MPs are still not clear.

The discovery of oceanic gyre-associated accumulation zones, so-called "garbage patches",[15] also stimulated intensified research efforts. Five such systems were confirmed to date and the suspected presence of further accumulation zones in the Arctic[16] was recently corroborated.[17] Cózar et al. reported increasing plastic concentrations toward the northernmost borders of the Greenland Sea due to the barrier imposed by the ice sheet.[17] One of these zones west of Svalbard happens to be close to the HAUSGARTEN observatory, from which increasing litter quantities were recorded on the deep seafloor between 2002 and 2014.[18,19] Litter and MP were also recorded from the nearby sea surface.[20,21] In addition, Arctic sea ice contains vast quantities of MPs (Peeken, unpubl. data).[22] Tekman et al. reported increasing numbers of smaller-sized plastic items (<10 cm) on the deep seafloor.[19] Although the deep seafloor may constitute a major sink for MP until now only three studies were dedicated to MP in deep-sea sediments at depths between 1,000−5,800 m from the Nile Deep Sea Fan, Southern Ocean, Porcupine Abyssal Plain, Mediterranean Sea, SW Indian Ocean, NE Atlantic Ocean and the NW Pacific Kuril-Kamchatka Trench.[23−25]

The aim of this study is to quantify MP pollution on the Arctic seafloor in the HAUSGARTEN observatory along a bathymetric transect ranging from 2500−5500 m depth. Sediments taken along a latitudinal gradient were also analyzed to assess the importance of MP release due to melting processes in the marginal ice zone. To attempt source allocation, the polymer composition of all particles identified is described and compared. In the absence of a standard operation procedure for the analysis of MP from sediments,[5] a new method was adopted to remove organic material (Fenton's reagent) prior to analysis by Fourier-transform infrared (FTIR) spectroscopy.[26]

MATERIALS AND METHODS

Study Area. The sediments analyzed during this study were taken from the Long-Term Ecological Research (LTER) observatory HAUSGARTEN in the summer of 2015 during expedition ARK 29.2 of the research icebreaker RV *Polarstern*. HAUSGARTEN was established by the Alfred Wegener Institute Helmholtz Centre for Polar and Marine Research in 1999 in the Fram Strait at N79°, west of Svalbard (Norway). It currently comprises 21 sampling stations along a latitudinal and a bathymetric gradient between 250−5500 m water depth.[27] These stations are subject to annual sampling campaigns targeting all ecosystem compartments from the sea surface to the deep seafloor. The Fram Strait represents the only deep-water connection between the North Atlantic and the Arctic Ocean. The HAUSGARTEN area is affected by warm Atlantic waters transported by the West Spitsbergen Current in the upper 500 m, which is fed by north Atlantic waters, such that the area is ice-free for most of the year. Still, the northern HAUSGARTEN stations N3 and N5 are covered by ice during winter, but ice can also be present during summer when ice floes are carried from the Central Arctic into the Fram Strait by the Transpolar Drift.[19] Below the warm Atlantic water layer, there are low-temperature waters modified by polar water masses.[28]

Sediment Sampling. To obtain virtually undisturbed sediment samples, a video-guided multiple corer (MUC; Oktopus GmbH) holding eight cores of 100 mm diameter was used. Three stations were sampled along the latitudinal gradient (N5, N3, S3), which runs along the 2500 m isobath (Table 1, Figure 1). These include the northernmost station N5, which is located in the marginal ice zone. Six samples were taken at stations from the bathymetric gradient (HG-IV−IX: 2342−5570 m water depth), including the Molloy Deep, the deepest part of the Arctic Ocean (Table 1, Figure 1). Depending on availability, the top 5 cm of 3−6 sediment cores were sliced off with a metal spatula and frozen in tin foil. Three additional samples were taken from different MUC cores with cutoff syringes and analyzed at 1 cm intervals down to 5 cm sediment depth. The bulk pigments registered by this method are termed chloroplastic pigment equivalents and indicate phytodetrital input to the seafloor.[29] They were extracted in 90% acetone and measured with a Turner fluorometer.[30,31]

In the laboratory, frozen sediments from all the cores of each station were defrosted, pooled and homogenized. Before the separation, the dry weight was determined by weighing three subsamples from each sample before and after drying at 60 °C.

Sediment Characterization and Separation. The Micro-Plastic Sediment Separator (MPSS; HYDRO-BIOS GmbH) was used to separate the denser sediment particles from the less dense MP particles.[32] A $ZnCl_2$ solution (1.7−1.8 g cm^{-3} density) was filtered into the MPSS using cartridge filters (10 μm stainless steel and 1 μm pleated PP; Wolftechnik Filtersysteme GmbH & Co. KG) each time prior to the addition of sediments. A steel rotor on the bottom of the MPSS mixed the sediment at ∼12 rpm for 35−60 min. The MPSS was filled to the lower half of the dividing chamber after the rotor had been turned off to avoid overflow of the sample. After 12 h, the MPSS was filled up to the upper part of the dividing chamber and left for 7 h. Finally, the ball valve between the two dividing chambers was closed and the $ZnCl_2$ solution above the ball valve was rinsed with Milli-Q into a glass bottle with glass cap and stored at 4 °C until further analysis.

Preparation of the Samples Prior to Analysis. A filtration step was required to remove the $ZnCl_2$ solution and to separate the sample into particle size fractions larger and smaller than 500 μm since μFTIR analysis in transmission mode can only identify particles <500 μm successfully. For this, each sample was at first filtered onto a 500-μm steel filter, using a vacuum filtration unit and rinsed several times with Milli-Q and 30% ethanol. The filtrate was then filtered onto a 20-μm stainless steel filter. If necessary, an ultrasonic bath (max. five min; 215 W; Sonorex RK514; Bandelin Electronic GmbH & Co. KG) was applied for 1−5 min to remove all particles left on the respective filters. Residual particles of both fractions were stored separately in glass flasks with Milli-Q.

Large Size Fraction (>500 μm). The large size fraction was sorted using a stereomicroscope (Olympus SZX16) and Bogorov chamber (10.5 × 7.3 cm) before analysis by attenuated total reflection Fourier-transform infrared spectroscopy (ATR-FTIR) of suspect MP particles. Each sample was assessed at 16-fold and some particles even at 32-fold magnification. Generally, particles of clear and homogeneous coloration and without cellular or organic structure were selected for analysis by ATR-FTIR.[33] The size of all particles

DOI: 10.1021/acs.est.7b03331
Environ. Sci. Technol. 2017, 51, 11000−11010

Table 1. Details of Sediment Sampling at HAUSGARTEN Stations, Biogeochemical Parameters and Prevailing Summer Sea Ice Conditions

	S3	HG-IV	HG-V	HG-VI	HG-VII	HG-VIII	HG-IX	N3	N5
sampling cast	PS93/48−11	PS93/50−19	PS93/51−4	PS93/53−3	PS93/54−2	PS93/55−2	PS93/56−1	PS93/85−2	PS93/60−10
date (dd/mm/yy)	25/07/15	27/07/15	28/07/15	28/07/15	29/07/15	29/07/15	29/07/15	11/08/15	03/08/15
latitude (N)	78°35,98′	79°04,91′	79°03,81′	79°03,61′	79°03,63′	79°3,86′	79°08,02′	79°36,25′	79°56,28′
longitude (E)	5°04,07′	4°08,59′	3°39,46′	3°34,98′	3°28,56′	3°20,10′	2°50,58′	5°10,28′	3°11,60′
depth (m)	2,342	2,460	3,127	3,430	4,092	5,108	5,570	2,783	2,549
mean ice concentration (%)	0.00	0.79	0.79	0.79	0.79	2.61	2.61	3.47	35.33
duration of ice coverage (days)	0	2	2	2	2	8	8	13	84
porosity (%)	60.54	53.86	51.01	47.26	42.34	36.91	60.72	58.97	60.48
chlorophyll *a* (μg cm^{-3})	1.25	1.38	1.42	1.30	1.38	1.45	1.11	n.a.	1.33
chloroplastic pigment equivalent (μg cm^{-3})	13.19	15.40	14.73	13.86	14.03	17.53	18.35	n.a.	17.71
particulate organic carbon (%)	0.78	0.66	0.74	0.61	0.59	0.68	1.09	0.88	0.88
phospholipids (nmol ml^{-1})	4.75	20.53	51.81	16.01	9.63	6.67	10.22	33.76	8.53

was determined by measuring the longest dimension with the cellSens software (Olympus). Currently, fibers cannot be well discerned by the applied Fourier-transform infrared microscopy (μFTIR) analytical method, which was used for the small size fraction (s. below). Therefore, they were also omitted in the analysis of particles of the large size fraction.

Small Size Fraction (<500 μm). While previous studies relied on enzymatic digestion, H_2O_2, acid or alkaline treatments to reduce organic material prior to spectroscopic analysis[34−36] Fenton's reagent ($FeSO_4$ in combination with H_2O_2) was recently suggested as a promising alternative agent.[26] The small size fraction was thus treated with Fenton's reagent to remove organic matter prior to μFTIR analysis. Briefly, a 7.2 mM $FeSO_4$ solution (pH < 5) was prepared by adding 1 g $FeSO_4$ to 50 mL Milli-Q. The sample was filtered onto a steel filter (20 μm) and placed into a beaker in a water bath (20 °C) and 10 mL $FeSO_4$ solution were added. Subsequently, 20 mL of H_2O_2 (30%) were added slowly. After 15 min, the filter was rinsed and subject to an ultrasonic bath (max. five min; 215 W) to remove residual particles on the filter. The samples were analyzed using the FlowCam (Fluid Imaging Technologies, Inc.) to visualize and quantify particle amounts and sizes and thereby a potential area coverage. Based on this assessment a certain volume of the sample, ranging between 1.3−67.7% was filtered onto an aluminum oxide (Anodisc) filter for μFTIR analysis.

Analyses by FTIR Spectroscopy. ATR-FTIR spectroscopy was used for the analysis of suspect single particles from the large size fraction (>500 μm) using a Tensor 27 spectrometer (Bruker Optics GmbH) including a platinum ATR unit (wavenumber range: 400−4,000 cm^{-1}, 4 cm^{-1} resolution, 6 mm aperture, 32 scans). After measurement, the spectrum was compared against reference spectra through a library search with the software Opus 7.5. Particles with a hit quality above 700 (max. of 1000 hit quality) were accepted as verified polymers. The library is available upon request.

The small size fraction (<500 μm) was measured by a TENSOR 27 spectrometer (Bruker Optics GmbH) connected to a Hyperion 3000 μFTIR microscope equipped with a focal plane array (FPA) detector with 64 × 64 detector elements. An infrared range of 1250−3600 cm^{-1} was used for measurements. Six scans were performed per field at a resolution of 8 cm^{-1} and a binning factor of 4 (see[37] for setting details).

After drying for at least 2 days (30 °C) the filter was placed under the FTIR-microscope onto a calcium fluoride window and an overview image was recorded. Subsequently, the concentrated filter area (166 mm^2, 73 × 73 FPA fields, 1.36 million spectra) was measured, which took ca. 13 h.

Automated Analysis of μFTIR Data. The data were processed by automated analyses of μFTIR data.[38] Briefly, each spectrum in the measurement file was analyzed via two library searches to confirm polymer identity. The library is available upon request. Each pixel identified was stored with its position, analysis quality and polymer type into a file, which was subject to image analysis based on Python 3.4 scripts and Simple ITK functions.[38] This combination enabled the identification, quantification and size determination of all polymer particles in a sample and additionally excluded human bias.[38] To reduce the complexity of the size distribution the analysis introduced size classes (for details see[38]).

Contamination Protection. If not stated otherwise all laboratory ware used was made of glass or stainless steel and thoroughly rinsed with Milli-Q before use. All polymer-based

DOI: 10.1021/acs.est.7b03331
Environ. Sci. Technol. 2017, 51, 11000−11010

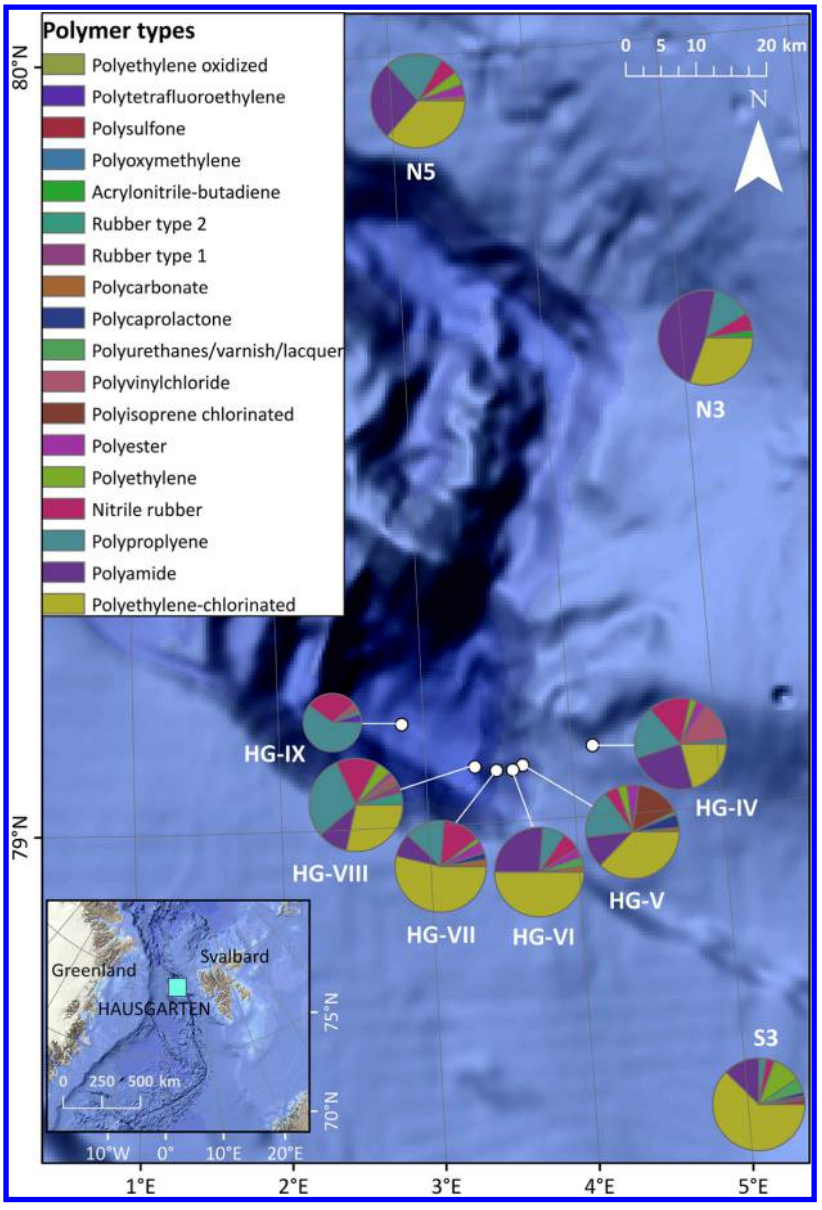

Figure 1. Abundance and composition of microplastics detected in sediments from the Artic deep sea (log scale, see Table 2 for abundance data).

items, which could not be replaced by alternative glass items (e.g., bottle caps, filter holders) were made of polytetrafluoroethylene (PTFE). Dustboxes (DB1000, G4 prefiltration, HEPA-H14 final filtration, Q = 950 m^3/h, Möcklinghoff Lufttechnik), which filter airborne particles, were installed in laboratories for density separation, particle sorting and FTIR analyses. All filtration steps were performed in a laminar flow cabinet (Scanlaf Fortuna, Labogene), except for the $ZnCl_2$ filtration by cartridge filter, to prevent airborne contamination. All chemicals (e.g., $FeSO_4$, H_2O_2) were filtered through polycarbonate filters (0.2 μm pore size, Merck Millipore, Isopore GTTP) to remove particulate contaminants before usage. To remove contaminants from the MPSS it was filled with $ZnCl_2$ and left to settle for 5 h. The upper layer of the $ZnCl_2$ solution (above the ball valve) was discarded prior to the addition of the next sample. Cotton laboratory coats were generally worn to reduce contamination from synthetic textiles. Latex gloves were worn for safety at work. To account for possible process contaminations in the evaluation of the samples, a procedural blank was run. For this purpose, an empty glass jar was rinsed with $ZnCl_2$ into the MPSS instead of adding sediment and all the following procedures (filtration, purification and analysis) were performed in the same way as for the other samples. The amounts of MPs determined in the samples were blank-corrected by calculating the amount of MPs in 100% of the sample volume (volume of samples analyzed by μFITR: S3 = 1.99%; HG-IV = 3.62%; HG-V = 1.84%; HG-VI = 2.29%; HG-VII = 3.96%; HG-VIII = 4.21%; HG-IX = 67.7%; N3 = 1.25%; N5 = 1.85%) and subtracting the amount of MPs determined in 100% of the blank. The number of particles kg^{-1} was calculated for each sample based on the amount of dry sediment.

Sea-Ice Concentration. To test for a correlation between the presence of sea ice above the sample location and MP deposition, sea-ice concentration data were obtained by the Centre for Satellite Exploitation and Research (CERSAT) at the Institut Français de Recherche pour l'Exploitation de la Mer (IFREMER), France.[39] The ice concentration was calculated based on the ARTIST Sea Ice (ASI) algorithm developed at the University of Bremen, Germany.[40] Sea-ice concentration data

DOI: 10.1021/acs.est.7b03331
Environ. Sci. Technol. 2017, 51, 11000−11010

Table 2. Microplastic Abundance (Number), Diversity (Shannon-Winer *H*) and Composition in Sediments from Different HAUSGARTEN Stations[a]

	S3	HG-IV[b]	HG-V	HG-VI	HG-VII	HG-VIII	HG-IX	N3[b]	N5	blank (>500 μm)	blank (<500 μm)
total MP abundance kg^{-1}	4520.22	4049.87	5568.02	2834.03	3855.99	5390.67	41.76	6594.56	6348.27	0	114
MP abundance (>500 μm) kg^{-1}	1.28	9.15	3.20	7.11	2.95	9.43	1.99	0.98	0.89		
total MP abundance cm^{-2}	11.52	7.05	15.23	8.92	16.97	24.74	0.32	17.32	15.26		
total MP abundance L^{-1}	2303.98	1409.95	2088.91	1222.90	3394.63	3392.98	44.43	3463.71	3051.60		
polymer diversity (H)	0.58	0.83	0.79	0.67	0.68	0.80	0.57	0.67	0.75		
polyethylene chlorinated	2816.02	827.05	2071.59	1413.70	2025.78	1513.71		1960.15	2311.53		10
polyamide	576.06	965.59	605.68	742.16	315.62	558.09		3071.23	1738.57		2
polypropylene	114.51	741.29	939.21	232.69	532.81	1557.57	25.15	855.96	1247.09		11
nitrile rubber	128.58	589.61	260.95	186.25	503.63	783.97	11.76	394.00	386.75		
polyethylene	456.76	99.85	188.93		60.03	271.15		34.47	298.16		45
polyester		136.44	227.34	94.31	152.36	69.79		58.11	271.28		21
polyisoprene chlorinated			869.83								
polyvinyl chloride		544.44			35.83	132.51	1.90				2
polyurethanes/varnish/lacquer	235.41	16.20	59.77	100.00	24.75	6.37		62.05			17
polycaprolactone	63.01		259.35		92.53	21.46					1
polycarbonate		37.54	82.18	57.82	91.05	64.37			94.00		3
rubber type 1	64.29				18.65	156.79					
rubber type 2						223.05	0.95				1
acrylonitrile-butadiene								157.60			
polyoxymethylene		82.70									1
polysulfone	64.29										
polytetrafluoroethylene	1.28	9.15	3.20	7.11	2.95	9.43	1.99	0.98	0.89		
polyethylene oxidized						22.40					

[a]To enable comparisons total MP kg^{-1} was converted to MP per area and volume. Polymer abundance in the samples refers to number kg^{-1} dry sediment of the sample; polymer abundance in the blank refers to 100% sample volume of the blank. All values are procedural blank corrected. [b]slight sample loss.

from all HAUSGARTEN stations (Table 1) were extracted for the summer months (May–July 2015) over an area of 12.5 × 12.5 km. From this, the mean summer ice concentration and the days of sea ice coverage were calculated for each station.

Data Analysis. The MP counts of the large and small size fractions were combined for data analyses. Since different sediment quantities were sampled from different stations the data were converted to MP kg^{-1}. In the current absence of established standards, MP counts were additionally converted to MP L^{-1} and MP cm^{-2} to enable comparison with published data given per unit volume and area although the latter may introduce variability because of differences in the sample volumes used. The polymer composition and MP particle size distribution of the different samples was compared by hierarchical cluster analysis (PRIMER-e version 6.1.6) based on group average linkage of Bray–Curtis similarity of square-root transformed polymer abundance data.[41] Polymer diversity was computed based on Shannon–Wiener diversity (log base e). We tested for Pearson's correlations between chlorophyll *a* content (mean of the 5 cm sections) and MP quantity as well as polymer diversity after establishing a normal distribution of the data using Anderson-Darling tests (Minitab 14; $p > 0.05$). Mean summer ice concentrations and number of days of sea ice coverage were used for Spearman's rank correlation tests with MP quantities and diversity for each station (Minitab 14).

RESULTS

Microplastic Quantities. MPs were detected in all sediment samples with an overall mean number of 4,356 (±675 standard error) particles kg^{-1} sediment. The highest numbers were found at the two northern stations N3 (6595 MPs kg^{-1}) and N5 (6348 MPs kg^{-1}), followed by HG-V (5568 MPs kg^{-1}), HG-VIII (5390 MPs kg^{-1}), the southernmost station S3 (4520 MPs kg^{-1}), HG-IV (4050 MPs kg^{-1}), HG-VII (3856 MPs kg^{-1}), HG-VI (2834 MPs kg^{-1}) and last by the deepest station HG-IX (42 MPs kg^{-1}) (Figure 1; Table 2). It should be noted that the MP counts from HG-IV and N3 may be slightly underestimated due to slight sample loss during preparation. All results presented are blank corrected.

Polymer Composition. Eighteen different polymer types were identified in total from all sediment samples (Table 2). In the larger size fraction (>500 μm), 177 potential plastic particles were analyzed, of which 31 were identified as plastic polymers (17.5%). The remaining particles could not be identified as they had a hit quality below 700 except for one cellulose particle and a particle identified as wild boar. While all plastics in this size fraction were identified as polytetrafluoroethylene (PTFE), there was great variability in the polymer composition in the small size fraction (<500 μm) with 18 different types found in total ranging between 5 (HG-IX) and 14 (HG-VIII) types per sample (Table 2). Since PTFE cannot be detected within the spectral region of 3600–1250 cm^{-1} available for the particles <500 μm in μFTIR, no statement on the presence or absence of PTFE in the small size fraction can be made. The polymer composition of the deepest station HG-IX, which was dominated by polypropylene (Figure 2) and nitrile rubber shared only 11% similarity with the other stations (Supporting Information (SI) Figure S1). The southernmost

DOI: 10.1021/acs.est.7b03331
Environ. Sci. Technol. 2017, 51, 11000–11010

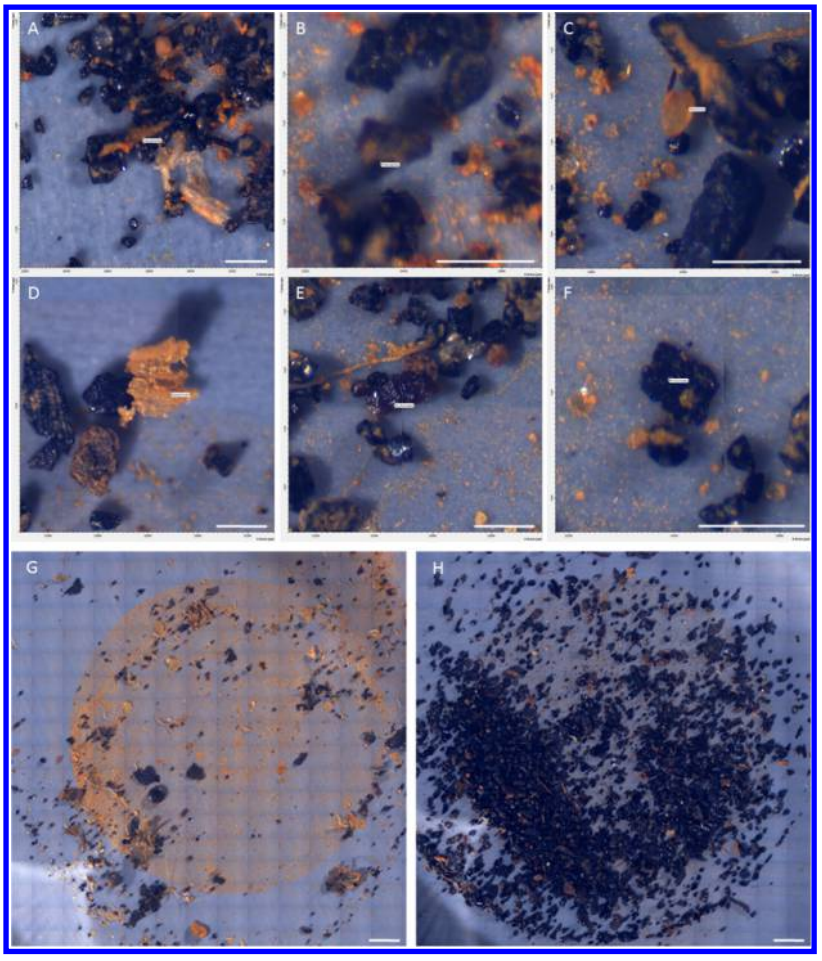

Figure 2. Panel showing examples of microplastic particles and an overview over exemplary samples. (A) Polycarbonate; (B) polypropylene; (C) polyurethane/varnish; (D) polycarbonate; (E,F) chlorinated polyethylene; scale bar A-F: 200 μm; (G) overview of sample HG-IX; (H) overview of sample HG-VII with many coal particles; scale bar G,H: 1 mm.

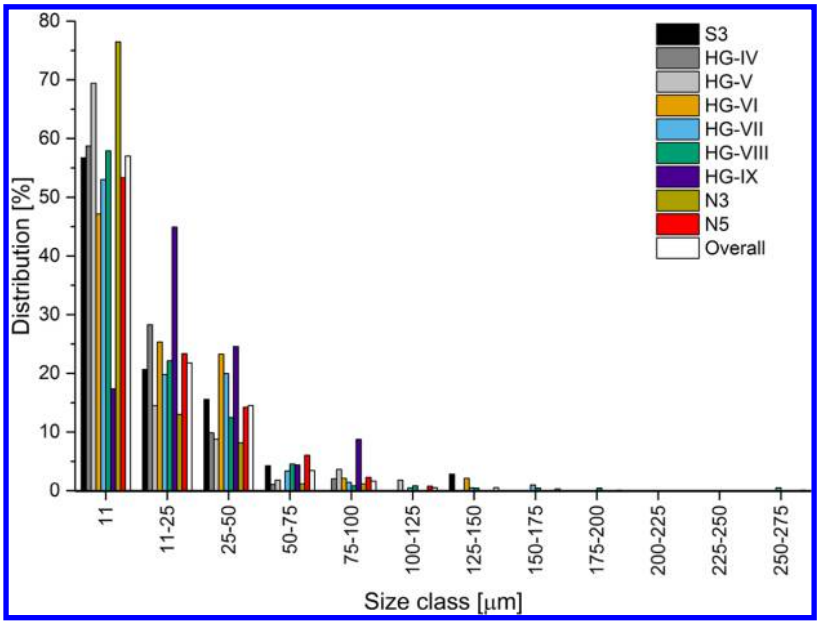

Figure 3. Size frequency distribution of all particles detected in all nine samples of the small size fraction (<500 μm).

station, S3, harbored a polymer composition, which was 63% similar to the remaining samples (SI Figure S1) and characterized by a great proportion (62%) of chlorinated polyethylene. The remaining samples had a 70−80% similar polymer composition (SI Figure S1). Polypropylene, nitrile rubber and PTFE occurred in all samples but polyamide and

DOI: 10.1021/acs.est.7b03331
Environ. Sci. Technol. 2017, 51, 11000−11010

chlorinated polyethylene were also detected in eight out of nine samples. In terms of overall particle numbers from all stations, chlorinated polyethylene accounted for the largest proportion (38%), followed by polyamide (22%), polypropylene (16%) and nitrile rubber (8%) (Table 2). This is also reflected in the polymer composition from different stations as summarized in Figure 1.

Black Particles. The small size fractions were characterized by numerous black particles (Figure 2), which proved to be coal. Unfortunately, the particle number could not be determined because single particles could not be distinguished by the algorithm used. Still, visual inspection implied that HG-VIII had the highest number of coal particles whereas samples from HG-IX (Figure 2) and S3 contained only few of these.

Polymer Size. Some 78% of all detected MPs were ≤25 μm and some 99% of all particles were smaller than 150 μm (Figure 3). Overall, the amount of particles decreased with increasing size. The size frequency of MP from HG-IX appeared to be slightly different from the other stations as the majority of particles was in the 11−25 μm size range (Figure 3). By contrast, all other stations had the highest frequency in the smallest size class.

Correlation between MP and Environmental Factors. There was no significant correlation between depth and MP abundance (SI Table S1), but surprisingly, MP abundance was positively correlated with chlorophyll *a* content (ρ = 0.78; p = 0.024). There was no significant correlation between MP abundance and sea ice concentration or days of ice coverage above the respective stations although the correlation was only just not significant (ρ = 0.66, p = 0.055). However, it should be noted that some of the stations are located closely together (ca. 17 km from HG-IV to HG-VII with 1.5−10 km distance between individual stations). As this is below the 12-km resolution of satellite imagery, these stations had the same ice concentration values, which may have resulted in nonsignificant correlations. Polymer diversity (Shannon−Wiener H) was also significantly positively correlated with chlorophyll *a* content (ρ = 0.95; p < 0.0001).

DISCUSSION

This study provides novel data on the contamination of Arctic deep-sea sediments, indicating higher MP abundance in the Fram Strait than in all other benthic regions investigated to date. Our methodological approach allowed us to detect unexpectedly high numbers of microplastics in sediments from the deep Fram Strait (42−6595 MPs kg^{-1}), especially in the small size range. While differences in sampling and analytical methodologies make straight comparisons with previous studies difficult, magnitude-scale comparisons may be legitimate. Most studies on sublittoral sediments from other regions of the world recorded lower numbers of MP particles than this study. For example,[23] reported MP quantities, which were 16 times lower from the deep Atlantic Ocean and Mediterranean Sea even if our lowest MP number from HG-IX was considered (0.02[23] vs 0.32 MPs cm^{-2} at HG-IX), although a comparison based on a conversion from volume to area metrics has to be treated with caution. Fewer MPs were also detected in the sediments from the deep NE Atlantic, Mediterranean and SW Indian Ocean although only fibers were considered (24−800 MP L^{-1} vs 44−3393 MP L^{-1} at HG).[25] Even the two subarctic samples taken nearby, SW of Svalbard, also had much lower concentrations ([25] converted: 0.002−0.003 L^{-1}). Lower MP levels were also recorded from the Kuril-Kamchatka Trench (NW Pacific) although very different sampling and analytical techniques were used.[24]

Recent data from Antarctic sediments indicate also much lower levels of MP contamination (converted: 0.0005−0.1705 cm^{-2}) although, these figures also include plastic particles >5 mm (~22%).[42] Sediments collected at 15 locations along the densely populated areas off the Belgium shelf (100−3600 MPs kg^{-1})[43] and the Dutch North Sea coast (54−3146 MPs kg^{-1})[44] approached more similar MP quantities as did sediments from the Venice Lagoon in Italy (2,175 MPs kg^{-1})[45] and the Belgian coast (390 MPs kg^{-1}).[46]

Still, overall the abundance of MP in the deep Fram Strait appears to be higher than in all other benthic regions investigated. Some of the observed differences may be due to differences in the methodology used. Unlike coring devices, for example, grabs produce a bow wave when lowered to the seafloor, which flushes the top sediment layer aside[48] preventing the detection of recently deposited pollutants. In addition, the MPSS recovers significantly more MP compared with other separation methods, especially in the small size range.[37] All of the above studies relied on the analysis of visually preselected particles. Our data showed, however, that nearly 80% of the MPs were smaller than 25 μm. This significant proportion would have gone unnoticed leading to serious underestimates. Despite these methodological differences the high abundance of microplastics in the deep-sea sediments of the remote Arctic Ocean is striking.

Still, even if a more sensitive methodological approach allowed us to detect higher MP quantities the magnitude of the differences indicates that HAUSGARTEN may be in or close to a plastic accumulation area. Similar MP numbers were recorded near the sea surface southwest of Svalbard using an underway sampling device and visual preselection ([21] converted: 2,680 MP L^{-1}). Recently, high numbers of small plastic debris were also reported from the sea surface in the Fram Strait pointing to an accumulation area south of HAUSGARTEN.[17] It was suggested that a significant fraction of this debris likely originated from Northern Europe and was transported to the North with the Thermohaline Circulation. Still, inputs from local sources may increasingly also contribute to this since anthropogenic activities such as fisheries and tourism have increased markedly due to the receding sea ice.[19] Plastic debris from fisheries nowadays dominates on the beaches of Svalbard.[47] The release of MP entrained in Arctic sea ice during melting processes[22] in the region can be considered another reason for the high MP quantities recorded although this has to be verified, for example, by analysis of samples from year round moored particle traps.[48]

Differences between HAUSGARTEN Stations. The two northernmost HAUSGARTEN stations N3 and N5 contained the highest MP numbers. Both stations are located within or close to the marginal ice zone, as shown by the highest ice concentration and duration of sea ice coverage. Arctic sea ice entrains enormous quantities of MP[22] during ice formation in the Central Arctic and may act as transport vehicle: after the ice breaks up in the Central Arctic in spring it is transported to the south as ice floes with the Transpolar Drift. On route, it encounters warmer Atlantic surface waters and continues to melt possibly releasing entrained MPs. Depending on the sinking velocity, there may be some horizontal displacement of particles from their point of origin at the sea surface as they descend to the seafloor. However,[49] reported fast sinking rates for some MP implying reasonably small catchment areas.

DOI: 10.1021/acs.est.7b03331
Environ. Sci. Technol. 2017, 51, 11000−11010

Increasing numbers of small plastic fragments (<10 cm) were also recorded on seafloor photographs at N3.[19] The number of MP at the two northern stations may thus be higher because they receive MP from meltwater as well as distant sources through the Thermohaline Circulation.

The other HAUSGARTEN stations may harbor a lower MP load because they receive MPs primarily only through the Thermohaline Circulation, whereas the northern stations are affected by both Atlantic waters and meltwater carrying MPs. The positive correlation between MP levels and chlorophyll *a* content suggests that Algae play a role in the downward transport. It should be noted that there was no significant correlation with total phytodetrital input, which also includes phaeophytin, an indicator of refractory material. This highlights the potential role of freshly deposited algal rather than older material. Indeed, the vertical transport of originally positively buoyant MPs may be accelerated significantly by the presence of aggregating Algae.[50,51] In the study area, the ice algal diatom *Melosira arctica* forms dense aggregates beneath the sea ice. During melting, such aggregates may entrain MP and rush to the deep seafloor[52] facilitating the deposition of MPs. In addition, Atlantic waters carry increasing amounts of the colony forming algae *Phaeocystis pouchetii* to HAUSGARTEN[27,48] whose polysaccharide gel matrix may entrain buoyant MP, too.

The low quantities of MP in the Molloy Deep, the deepest depression of the Arctic, were surprising. If nothing else, higher MP levels were expected because of the funnel-shaped surrounding topography and the presence of downward directed eddy systems, all favoring the accumulation of MPs. It could be argued that MP export is attenuated with depth as is the vertical export of particulate organic matter.[53] However, the third highest MP concentration recorded at the nearby station HG-VIII at similar depth (5,100 m, 12 km distance) contradicts this notion. Another possibility is that MPs have evaded our detection because they were already incorporated in an exceptionally high standing stock of infaunal meiofauna[54] and epibenthic megafauna, which distinguishes this station and consists primarily of the deposit-feeding sea cucumber *Elpidia heckeri*.[55] Recently, epibenthic megafauna including sea cucumbers from the deep SW Indian Ocean and equatorial mid-Atlantic were shown to ingest MP.[56] Microplastic abundance in North Sea and English Channel sediments was influenced by other factors including carbon content and grain size.[44] By contrast, at HAUSGARTEN, neither organic carbon content nor porosity appeared to be correlated with MP numbers. Of the parameters tested, only chlorophyll *a* and marginally possibly also summer sea-ice concentration appeared to be correlated although low sample sizes may have obscured possible correlations. As stated above, this could be seen as an indication of enhanced vertical transport via incorporation in fast-sinking ice-algal aggregates. Still, samples from the water column or experimental work are required to establish mechanistic links. In addition, further benthic studies are needed to assess if the wider Arctic region is contaminated with MP or if the Fram Strait area is an accumulation zone.

Particle Composition. Polypropylene, nitrile rubber, and PTFE occurred in all samples but polyamide and chlorinated polyethylene were also detected in eight out of nine samples. In terms of overall particle numbers from all stations, chlorinated polyethylene accounted for the largest proportion (38%), followed by polyamide (22%), polypropylene (16%), and nitrile rubber (8%). Since the density of PTFE (2.10−2.30 g cm^{-3}),[57] nitrile rubber (1.30 g cm^{-3}) and polyamide (1.13 g cm^{-3}) exceeds the density of seawater (1.02−1.03 g cm^{-3})[4] these MPs are likely to sink to the seafloor directly. By contrast, polypropylene and chlorinated polyethylene have a lower density[4] such that a combination of processes including eddies and wind mixing,[58] biofouling, incorporation in sinking aggregates and vertical transport with biota or faeces must counteract their buoyancy. Polypropylene and polyethylene are the most widely demanded plastic types in Europe[59] and widely used for e.g. packaging and fishing gear.[4] Therefore, its prevalence does not come as a surprise. These two polymer types accounted also for almost half of the MPs from Atlantic surface waters.[57] Microplastics from surface waters southwest of Svalbard contained polyester (15%), polyamide (15%), acrylic (10%), polyethylene (5%), and polyvinyl chloride (5%).[21] Polyethylene and to a lesser degree also polyamide dominated MP in Arctic sea ice sampled in 2014, one year before our sediment sampling, especially in the two cores from the Fram Strait (Peeken, unpubl. data). All polymers detected in the ice cores or surfaces waters of the Arctic Ocean (except acrylic) have been also detected in the deep-sea sediments of the Arctic Ocean. This indicates that both surface waters and sea ice are possible sources of MP found in the sediment at HAUSGARTEN. Only few previous studies analyzed the composition of the polymers identified. Polyester followed by acrylic fibers dominated in sediments from the deep NE Atlantic, Mediterranean, SW Indian Ocean samples and subarctic sites.[25] Central Arctic ice cores were also characterized by a different MP composition, which was dominated by polyester (21%) and nylon/polyamide (16%), polypropylene (3%), and then by 2% each of polystyrene, acrylic, and polyethylene.[22] Still, the majority of particles were fibers, which were not considered in the present study. Other studies on MP in the deep sea did not describe the polymer composition.[23,24] Unfortunately, the abundance of coal particles could not be determined but such particles were also reported before in deep-sea sediments between New Zealand and Antarctica (5314 m depth) and the Porcupine Abyssal Plain (4100 m depth)[60] as well as from the Arctic and Subarctic Ocean.[61] The latter was attributed to atmospheric deposition and fluvial discharge, as ice-rafted material, coastal erosion, and the adsorption of dissolved black carbon onto particles.

Polymer Size. Overall, 83% of the analyzed particles in the large size fraction (>500 μm) were not identified as polymers. This highlights once more a likely overestimation of MP particles when relying exclusively on visual identification.[37] At the same time, it cannot be excluded that some particles may be overlooked during the visual identification step leading to an underestimation.

The analysis of the particles in the large size fraction showed also differences compared to other studies reporting particles >500 μm. While other studies detected particles with striking colors as well as white, black, gray and translucent particles[62,63] only PTFE particles were identified in this study that were white, black or gray. By contrast, particles of a striking color were not identified as polymers showing once again the need for spectroscopic methods for a reliable identification of polymers.

As stated above, some 80% of the MPs were ≤25 μm. The size structure of MP particles was steadily increasing in numbers toward lower sizes with no sign of saturation toward the lower size end. This may indicate that deep-sea sediments contain even more particles in yet smaller particle sizes, which have evaded our detection and that of previous studies. In

DOI: 10.1021/acs.est.7b03331
Environ. Sci. Technol. 2017, 51, 11000−11010

Atlantic surface waters, the majority of MP particles (64%) detected were <40 μm.[57] Freezing and melting processes[17] as well as an increased exposure to sunlight during the Arctic summer may enhance fragmentation into smaller particles compared with other areas. Ingestion by benthic biota on the seafloor[56] may break up MP in the sediments, also leading to more small-sized particles.

The high incidence of small MPs concurs with recent evidence suggesting that smaller MP particles sink faster than larger ones because they have a greater surface area, which can be fouled reducing their buoyancy and thereby enhancing sinking velocity.[64] Modeling of the vertical dispersion of positively buoyant small and large MPs also suggests that smaller MPs sink more readily.[57] Fragmentation in particle sizes below our current detection ability and loss of MP from the sea surface as a function of decreasing size may explain some of the 99% discrepancy between current global estimates of plastics entering the ocean from land[2] and estimates derived from field data.[3]

Appraisal of Methodology. In this study, a density separation with the MPSS was performed, which has a higher recovery rate for MP particles (95.5 ± 1.8%)[32] than e.g. the classical density separation setup that is used by others.[5] The two-step filling of the MPSS was chosen since one sample (HG-IV) overflowed due to a reaction accompanied by gas development in the MPSS. Therefore, the results from this station likely underestimate the actual MP numbers.

The use of Fenton's reagent lead to a reduction of organic material in the Arctic deep-sea sediments. This relatively new purification method prior to spectroscopic analysis was chosen to remove the high amounts of refractory material. Other purification methods, e.g. enzymes,[34] were not expected to act as efficiently on the deep-sea sediments. In addition, Fenton's reagent has no visible influence on polymers.[65] It was simple to use, reduced the organic material at high speed and was inexpensive. Samples were analyzed by FlowCam analysis before Fenton's treatment. The high amount of coal particles mentioned above impeded the FlowCam analysis since many of these stuck to the funnel of the device and were therefore not detected. Hence, it was decided to base the sample volumes, which could be filtered onto Anodisc filters, onto the more conservative results from the analysis before purification. In total, the subsamples analyzed by μFTIR ranged from 1.3% (N3) to 67.7% (HG-IX) of the samples. The results were extrapolated to 100% of each sample assuming a homogeneous distribution of MPs in terms of quantity and composition. This could have introduced bias.

By the application of a μFTIR microscope combined with an FPA[66] the analysis of whole filter areas was possible (~13 h). The evaluation relied on a new automated analysis approach,[38] which reduces human bias and enabled the analysis of several samples in parallel. In addition, it allows a simultaneous quantification, identification and size determination of the MP particles present.

Our data show that MP nowadays prevails even in one of the remotest parts of our planet, the Arctic deep sea. Although methodological differences make a straight comparison of MP numbers from different studies difficult, HAUSGARTEN sediments are clearly among the most polluted benthic sediments reported to date. Recently, a plastic accumulation area was reported at the sea surface some 300 km south of the observatory.[17] It was suggested that plastic debris likely originated from distant sources and was carried from the north Atlantic to the North via the Thermohaline Circulation.[17] The highest numbers of MPs at the northernmost stations, which are located in the marginal ice zone may indicate an additional pathway of MP to the Fram Strait. MP entrained in sea ice from the central Arctic may be transported with ice floes via the Transpolar Drift to the Fram Strait, where it melts and releases its MPs. The mixing of water masses of different salinity and temperature as well as incorporation in fast-sinking algal aggregates and biofouling may facilitate deposition of MP on the deep seafloor.

Still, whatever the exact pathway of MP, it likely originated from distant sources highlighting once more the need for significantly improved international frameworks aimed at reducing the inputs of plastic waste into our oceans.

■ ASSOCIATED CONTENT

Supporting Information

The Supporting Information is available free of charge on the ACS Publications website at DOI: 10.1021/acs.est.7b03331.

Summary statistics of correlation tests between microplastic abundance (MP) as well as diversity and environmental parameters. Cluster analysis showing the similarity in the composition of polymers in sediments from different stations of the deep-sea observatory HAUSGARTEN (PDF)

■ AUTHOR INFORMATION

Corresponding Author

*E-mail: melanie.Bergmann@awi.de.

ORCID

Melanie Bergmann: 0000-0001-5212-9808

Notes

The authors declare no competing financial interest.

‖Shared first authors

■ ACKNOWLEDGMENTS

We thank the officers and crew of RV *Polarstern* and chief scientist of expedition PS93, T. Soltwedel. I. Schewe operated the multiple corer and C. Hasemann was in charge of biogeochemical sediment analyses, assisted by A. Pappert. MB was funded by the Helmholtz Alliance ROBEX (Robotic Exploration of Extreme Environments) and CL by a Ph.D. scholarship of the Deutsche Bundesstiftung Umwelt. This work was supported by the German Federal Ministry of Education and Research (Project BASEMAN - Defining the baselines and standards for microplastics analyses in European waters; BMBF grant 03F0734A) and contributes to the Pollution Observatory of the Helmholtz-funded infrastructure programme FRAM (Frontiers in Arctic Marine Research), which funded MBT. We value the comments of three reviewers, who improved an earlier version of this paper. This publication is Eprint ID 45112 of the Alfred-Wegener-Institut Helmholtz-Zentrum für Polar- und Meeresforschung.

■ REFERENCES

(1) Geyer, R.; Jambeck, J. R.; Law, K. L. Production, use, and fate of all plastics ever made. *Sci. Adv.* **2017**, *3* (7), e1700782.

(2) Jambeck, J. R.; Geyer, R.; Wilcox, C.; Siegler, T. R.; Perryman, M.; Andrady, A.; Narayan, R.; Law, K. L. Plastic waste inputs from land into the ocean. *Science* **2015**, *347* (6223), 768−771.

(3) van Sebille, E.; Wilcox, C.; Lebreton, L.; Maximenko, N.; Hardesty, B. D.; van Franeker, J. A.; Eriksen, M.; Siegel, D.; Galgani,

DOI: 10.1021/acs.est.7b03331
Environ. Sci. Technol. 2017, 51, 11000−11010

F.; Law, K. L. A global inventory of small floating plastic debris. *Environ. Res. Lett.* **2015**, *10* (12), 124006.
(4) Andrady, A. L., Persistence of plastic litter in the oceans. In *Marine Anthropogenic Litter*; Bergmann, M.; Gutow, L.; Klages, M., Eds; Springer: Berlin, Germany, 2015; pp 57−72.
(5) Hidalgo-Ruz, V.; Gutow, L.; Thompson, R. C.; Thiel, M. Microplastics in the Marine Environment: A Review of the Methods Used for Identification and Quantification. *Environ. Sci. Technol.* **2012**, *46* (6), 3060−3075.
(6) GESAMP *Sources, Fate and Effects of Microplastics in the Marine Environment: A Global Assessment*; IMO/FAO/UNESCO-IOC/UNIDO/WMO/IAEA/UN/UNEP/UNDP Joint Group of Experts on the Scientific Aspects of Marine Environmental Protection: 2015; p 96.
(7) Carpenter, E. J.; Smith, K. L. Plastics on the Sargasso Sea Surface. *Science* **1972**, *175* (4027), 1240−1241.
(8) Thompson, R. C.; Olsen, Y.; Mitchell, R. P.; Davis, A.; Rowland, S. J.; John, A. W. G.; McGonigle, D.; Russell, A. E. Lost at Sea: Where Is All the Plastic? *Science* **2004**, *304* (5672), 838.
(9) Lusher, A., Microplastics in the marine environment: distribution, interactions and effects. In *Marine Anthropogenic Litter*; Bergmann, M.; Gutow, L.; Klages, M., Eds; Springer: Berlin, Germany, 2015; pp 245−307.
(10) Bergmann, M.; Tekman, M. B.; Gutow, L. Marine litter: Sea change for plastic pollution. *Nature* **2017**, *544* (7650), 297−297.
(11) Hämer, J.; Gutow, L.; Köhler, A.; Saborowski, R. Fate of Microplastics in the Marine Isopod *Idotea emarginata*. *Environ. Sci. Technol.* **2014**, *48*, 13451−13458.
(12) Jani, P. U.; Florence, A. T.; McCarthy, D. E. Further histological evidence of the gastrointestinal absorption of polystyrene nanospheres in the rat. *Int. J. Pharm.* **1992**, *84* (3), 245−252.
(13) Brennecke, D.; Ferreira, E. C.; Costa, T. M. M.; Appel, D.; da Gama, B. A. P.; Lenz, M. Ingested microplastics (>100 μm) are translocated to organs of the tropical fiddler crab *Uca rapax*. *Mar. Pollut. Bull.* **2015**, *96*, 491−495.
(14) Farrell, P.; Nelson, K. Trophic level transfer of microplastic: *Mytilus edulis* (L.) to *Carcinus maenas* (L.). *Environ. Pollut.* **2013**, *177*, 1−3.
(15) Moore, C. J.; Moore, S. L.; Leecaster, M. K.; Weisberg, S. B. A comparison of plastic and plankton in the North Pacific Central Gyre. *Mar. Pollut. Bull.* **2001**, *42* (12), 1297−1300.
(16) van Sebille, E.; England, M. H.; Froyland, G. Origin, dynamics and evolution of ocean garbage patches from observed surface drifters. *Environ. Res. Lett.* **2012**, *7* (4), 044040.
(17) Cózar, A.; Martí, E.; Duarte, C. M.; García-de-Lomas, J.; van Sebille, E.; Ballatore, T. J.; Eguíluz, V. M.; González-Gordillo, J. I.; Pedrotti, M. L.; Echevarría, F.; Troublé, R.; Irigoien, X., The Arctic Ocean as a dead end for floating plastics in the North Atlantic branch of the Thermohaline Circulation. *Sci. Adv.*. **2017**, *3*, (e1600582).e160058210.1126/sciadv.1600582
(18) Bergmann, M.; Klages, M. Increase of litter at the Arctic deep-sea observatory HAUSGARTEN. *Mar. Pollut. Bull.* **2012**, *64*, 2734−2741.
(19) Tekman, M. B.; Krumpen, T.; Bergmann, M. Marine litter on deep Arctic seafloor continues to increase and spreads to the North at the HAUSGARTEN observatory. *Deep Sea Res., Part I* **2017**, *120*, 88−99.
(20) Bergmann, M.; Sandhop, N.; Schewe, I.; D'Hert, D. Observations of floating anthropogenic litter in the Barents Sea and Fram Strait, Arctic. *Polar Biol.* **2016**, *39* (3), 553−560.
(21) Lusher, A. L.; Tirelli, V.; O'Connor, I.; Officer, R. Microplastics in Arctic polar waters: the first reported values of particles in surface and sub-surface samples. *Sci. Rep.* **2015**, *5*, 14947.
(22) Obbard, R. W.; Sadri, S.; Wong, Y. Q.; Khitun, A. A.; Baker, I.; Thompson, R. C. Global warming releases microplastic legacy frozen in Arctic Sea ice. *Earth's Future* **2014**, *2* (6), 2014EF000240.
(23) van Cauwenberghe, L.; Vanreusel, A.; Mees, J.; Janssen, C. R. Microplastic pollution in deep-sea sediments. *Environ. Pollut.* **2013**, *182*, 495−499.
(24) Fischer, V.; Elsner, N. O.; Brenke, N.; Schwabe, E.; Brandt, A. Plastic pollution of the Kuril-Kamchatka-trench area (NW Pacific). *Deep Sea Res., Part II* **2015**, *111*, 399−405.
(25) Woodall, L. C.; Sanchez-Vidal, A.; Canals, M.; Paterson, G. L. J.; Coppock, R.; Sleight, V.; Calafat, A. M.; Rogers, A. D.; Narayanaswamy, B. E.; Thompson, R. C. The deep sea is a major sink for microplastic debris. *R. Soc. Open Sci.* **2014**, *1* (4), 140317.
(26) Tagg, A. S.; Harrison, J. P.; Ju-Nam, Y.; Sapp, M.; Bradley, E. L.; Sinclair, C. J.; Ojeda, J. J. Fenton's reagent for the rapid and efficient isolation of microplastics from wastewater. *Chem. Commun.* **2017**, *53* (2), 372−375.
(27) Soltwedel, T.; Bauerfeind, E.; Bergmann, M.; Bracher, A.; Budaeva, N.; Busch, K.; Cherkasheva, A.; Fahl, K.; Grzelak, K.; Hasemann, C.; Jacob, M.; Kraft, A.; Lalande, C.; Metfies, K.; Nöthig, E.-M.; Meyer, K.; Quéric, N.-V.; Schewe, I.; Włodarska-Kowalczuk, M.; Klages, M. Natural variability or anthropogenically-induced variation? Insights from 15 years of multidisciplinary observations at the arctic marine LTER site HAUSGARTEN. *Ecol. Indic.* **2016**, *65*, 89−102.
(28) Beszczynska-Möller, A.; Fahrbach, E.; Schauer, U.; Hansen, E. Variability in Atlantic water temperature and transport at the entrance to the Arctic Ocean, 1997−2010. *ICES J. Mar. Sci.* **2012**, *69* (5), 852−863.
(29) Thiel, H., Benthos in upwelling regions. In *Upwelling Ecosystems*; Boje, R.; Tomczak, M., Eds; Springer: Berlin, Germany, 1978; pp 124−138.
(30) Yentsch, C. S.; Menzel, D. W. A method for the determination of phytoplankton chlorophyll and phaeophytin by fluorescence. *Deep-Sea Res. Oceanogr. Abstr.* **1963**, *10* (3), 221−231.
(31) Holm-Hansen, O.; Lorenzen, C. J.; Holmes, R. W.; Strickland, J. D. H. Fluorometric determination of chlorophyll. *ICES J. Mar. Sci.* **1965**, *30* (1), 3−15.
(32) Imhof, H. K.; Schmid, J.; Niessner, R.; Ivleva, N. P.; Laforsch, C. A novel, highly efficient method for the separation and quantification of plastic particles in sediments of aquatic environments. *Limnol. Oceanogr.: Methods* **2012**, *10* (7), 524−537.
(33) Norén, F.; Naustvoll, L.-J. *Survey of microscopic anthropogenic particles in Skagerrak*; TA 2779−2011; Klima- og forurensningsdirektoratet TA: Lysekil and Flødevigen: Sweden, 2011; pp 1−20.
(34) Mintenig, S. M.; Int-Veen, I.; Löder, M. G. J.; Primpke, S.; Gerdts, G. Identification of microplastic in effluents of waste water treatment plants using focal plane array-based micro-Fourier-transform infrared imaging. *Water Res.* **2017**, *108*, 365−372.
(35) Claessens, M.; van Cauwenberghe, L.; Vandegehuchte, M. B.; Janssen, C. R. New techniques for the detection of microplastics in sediments and field collected organisms. *Mar. Pollut. Bull.* **2013**, *70* (1−2), 227−233.
(36) Tagg, A. S.; Sapp, M.; Harrison, J. P.; Ojeda, J. J. Identification and quantification of microplastics in wastewater using focal plane array-based reflectance micro-FT-IR imaging. *Anal. Chem.* **2015**, *87* (12), 6032−6040.
(37) Löder, M. G. J.; Gerdts, G., Methodology used for the detection and identification of microplastics − a critical appraisal. In *Marine Anthropogenic Litter*; Bergmann, M.; Gutow, L.; Klages, M., Eds; Springer: Berlin, Germany, 2015; pp 201−227.
(38) Primpke, S.; Lorenz, C.; Rascher-Friesenhausen, R.; Gerdts, G. An automated approach for microplastics analysis using focal plane array (FPA) FTIR microscopy and image analysis. *Anal. Methods* **2017**, *9* (9), 1499−1511.
(39) Ezraty, R.; Girard-Ardhuin, F.; Pioll, J. F.; Kaleschke, L.; Heygster, G., Arctic and Antarctic Sea Ice Concentration and Arctic Sea Ice Drift Estimated from Special Sensor Microwave Imager Data. 2007.
(40) Spreen, G.; Kaleschke, L.; Heygster, G. Sea Ice Remote Sensing Using AMSR-E 89 GHz Channels. *J. Geophys. Res.* **2008**, *113*, 1−14.
(41) Clarke, K. R.; Gorley, R. N., *Primer v6: User Manual/Tutorial*. Plymouth, UK, 2006; p 190.
(42) Munari, C.; Corbau, C.; Simeoni, U.; Mistri, M. Marine litter on Mediterranean shores: Analysis of composition, spatial distribution

DOI: 10.1021/acs.est.7b03331
Environ. Sci. Technol. 2017, 51, 11000−11010

and sources in north-western Adriatic beaches. *Waste Manage.* **2016**, *49*, 483−490.
(43) Leslie, H. A.; Brandsma, S. H.; van Velzen, M. J. M.; Vethaak, A. D. Microplastics en route: Field measurements in the Dutch river delta and Amsterdam canals, wastewater treatment plants, North Sea sediments and biota. *Environ. Int.* **2017**, *101*, 133−142.
(44) Maes, T.; van der Meulen, M. D.; Devriese, L. I.; Leslie, H. A.; Huvet, A.; Frère, L.; Robbens, J.; Vethaak, A. D. Microplastics Baseline Surveys at the Water Surface and in Sediments of the North-East Atlantic. *Front. Mar. Sci.* **2017**, *4* (135), 1−13.
(45) Vianello, A.; Boldrin, A.; Guerriero, P.; Moschino, V.; Rella, R.; Sturaro, A.; Da Ros, L. Microplastic particles in sediments of Lagoon of Venice, Italy: first observations on occurrence, spatial patterns and identification. *Estuarine, Coastal Shelf Sci.* **2013**, *130*, 54−61.
(46) Claessens, M.; Meester, S. D.; Landuyt, L. V.; Clerck, K. D.; Janssen, C. R. Occurrence and distribution of microplastics in marine sediments along the Belgian coast. *Mar. Pollut. Bull.* **2011**, *62* (10), 2199−2204.
(47) Bergmann, M.; Lutz, B.; Tekman, M. B.; Gutow, L., Citizen scientists reveal: marine litter pollutes Arctic beaches and affects Arctic wildlife. *Mar. Pollut. Bull.* under review.
(48) Lalande, C.; Bauerfeind, E.; Nöthig, E.-M. Downward particulate organic carbon export at high temporal resolution in the eastern Fram Strait: influence of Atlantic Water on flux composition. *Mar. Ecol.: Prog. Ser.* **2011**, *440*, 127−136.
(49) Khatmullina, L.; Isachenko, I. Settling velocity of microplastic particles of regular shapes. *Mar. Pollut. Bull.* **2017**, *114* (2), 871−880.
(50) Long, M.; Moriceau, B.; Gallinari, M.; Lambert, C.; Huvet, A.; Raffray, J.; Soudant, P. Interactions between microplastics and phytoplankton aggregates: Impact on their respective fates. *Mar. Chem.* **2015**, *175*, 39−46.
(51) Long, M.; Paul-Pont, I.; Hégaret, H.; Moriceau, B.; Lambert, C.; Huvet, A.; Soudant, P. Interactions between polystyrene microplastics and marine phytoplankton lead to species-specific hetero-aggregation. *Environ. Pollut.* **2017**, *228*, 454−463.
(52) Boetius, A.; Albrecht, S.; Bakker, K.; Bienhold, C.; Felden, J.; Fernández-Méndez, M.; Hendricks, S.; Katlein, C.; Lalande, C.; Krumpen, T.; Nicolaus, M.; Peeken, I.; Rabe, B.; Rogacheva, A.; Rybakova, E.; Somavilla, R.; Wenzhöfer, F. Export of algal biomass from the melting arctic sea ice. *Science* **2013**, *339* (6126), 1430−1432.
(53) Suess, E. Particulate organic carbon flux in the oceans-surface productivity and oxygen utilization. *Nature* **1980**, *288* (5788), 260−263.
(54) Soltwedel, T.; Miljutina, M.; Mokievsky, V.; Vopel, K. The meiobenthos of the Molloy Deep (5600 m), Fram Strait, Arctic Ocean. *Vie Milieu* **2003**, *53*, 1−13.
(55) Soltwedel, T.; Jaeckisch, N.; Ritter, N.; Hasemann, C.; Bergmann, M.; Klages, M. Bathymetric patterns of megafaunal assemblages from the arctic deep-sea observatory HAUSGARTEN. *Deep Sea Res., Part I* **2009**, *56* (10), 1856−1872.
(56) Taylor, M. L.; Gwinnett, C.; Robinson, L. F.; Woodall, L. C. Plastic microfibre ingestion by deep-sea organisms. *Sci. Rep.* **2016**, *6*, 33997.
(57) Enders, K.; Lenz, R.; Stedmon, C. A.; Nielsen, T. G. Abundance, size and polymer composition of marine microplastics $\geq$ 10 μm in the Atlantic Ocean and their modelled vertical distribution. *Mar. Pollut. Bull.* **2015**, *100* (1), 70−81.
(58) Kukulka, T.; Proskurowski, G.; Morét-Ferguson, S.; Meyer, D. W.; Law, K. L. The effect of wind mixing on the vertical distribution of buoyant plastic debris. *Geophys. Res. Lett.* **2012**, *39* (7), L07601.
(59) PlasticsEurope *Plastics-the Facts 2016*; Brussels, 2016.
(60) Masiello, C. A.; Druffel, E. R. M. Black Carbon in Deep-Sea Sediments. *Science* **1998**, *280* (5371), 1911−1913.
(61) Fang, Z.; Yang, W.; Chen, M.; Zheng, M.; Hu, W. Abundance and sinking of particulate black carbon in the western Arctic and Subarctic Oceans. *Sci. Rep.* **2016**, *6*, 29959.
(62) Stolte, A.; Forster, S.; Gerdts, G.; Schubert, H. Microplastic concentrations in beach sediments along the German Baltic coast. *Mar. Pollut. Bull.* **2015**, *99* (1−2), 216−229.
(63) Shaw, D. G.; Day, R. H. Colour- and form-dependent loss of plastic micro-debris from the North Pacific Ocean. *Mar. Pollut. Bull.* **1994**, *28* (1), 39−43.
(64) Fazey, F. M. C.; Ryan, P. G. Biofouling on buoyant marine plastics: An experimental study into the effect of size on surface longevity. *Environ. Pollut.* **2016**, *210*, 354−360.
(65) Oliveros, E.; Legrini, O.; Hohl, M.; Müller, T.; Braun, A. M. Industrial waste water treatment: large scale development of a light-enhanced Fenton reaction. *Chem. Eng. Process.* **1997**, *36* (5), 397−405.
(66) Löder, M. G. J.; Kuczera, M.; Mintenig, S.; Lorenz, C.; Gerdts, G. Focal plane array detector-based micro-Fourier-transform infrared imaging for the analysis of microplastics in environmental samples. *Env. Chem.* **2015**, *12*, 563−581.

DOI: 10.1021/acs.est.7b03331
Environ. Sci. Technol. 2017, 51, 11000−11010